

Vulcanized Vortex

Inyong Cho*

*Department of Physics and BK21 Physics Research Division,
Sungkyunkwan University, Suwon 440-746, Korea*

Youngone Lee†

Department of Physics, Daejin University, Pocheon, Gyeonggi 487-711, Korea

We investigate vortex configurations with the “vulcanization” term inspired by the renormalization of ϕ_\star^4 theory in the canonical θ -deformed noncommutativity. We focus on the classical limit of the theory described by a single parameter which is the ratio of the vulcanization and the noncommutativity parameters. We perform numerical calculations and find that nontopological vortex solutions exist as well as Q-ball type solutions, but topological vortex solutions are not admitted.

PACS numbers: 11.10.Lm, 11.10.Nx, 11.27.+d

I. INTRODUCTION

In the quantum theory of spacetime, we have noncommutative algebras of observables which correspond to commutative algebras in classical theory. Although we do not know the exact noncommutative algebra, or the commutation relations between related observables yet, studying some models of noncommutative spacetime would be instructive in that it gives some hints for true quantum spacetime physics.

Among many proposed noncommutative models, the canonical θ -deformed noncommutativity [1] and the κ -deformed noncommutativity [2] have been widely studied. Our work in this paper is based on the canonical noncommutative spacetime. The commutation relation between coordinates is given by

$$[x^\mu, x^\nu] = i\theta^{\mu\nu}, \quad (1)$$

where $\theta^{\mu\nu}$ is a constant antisymmetric matrix. By a suitable transformation, we can always write $\theta^{\mu\nu}$ in the form of

$$[\theta^{\mu\nu}] = \begin{pmatrix} 0 & \theta_E & 0 & 0 \\ -\theta_E & 0 & 0 & 0 \\ 0 & 0 & 0 & \theta_B \\ 0 & 0 & -\theta_B & 0 \end{pmatrix}, \quad (2)$$

which exhibits $\text{SO}(2) \times \text{SO}(2)$ structure.

Quantum field theory in this canonical noncommutative spacetime (NCQFT) has many characteristic aspects when compared to commutative theory. Among those aspects, the most significant pathology is the nonrenormalizability of the theory. Minwalla et.al. pointed out the mixing of different scales of the theory known as UV/IR mixing in the canonical NCQFT [3]. The perturbative analysis of the canonical NCQFT shows infinitely many infrared divergencies which cannot be reabsorbed to the parameters of the original theory.

This problem of nonrenormalizability has been recently resolved by Grosse and Wulkenhaar [4]. By adding the so-called “vulcanization” term to the action they could successfully show the renormalizability of the theory. The vulcanized action of the ϕ_\star^4 theory has the form,

$$S[\phi] = \int d^4x \sqrt{g} \left[\frac{1}{2} \partial_\mu \phi \star \partial^\mu \phi + \frac{\Omega^2}{2} (\tilde{x}_\mu \phi) \star (\tilde{x}^\mu \phi) + \frac{m^2}{2} \phi \star \phi + \frac{\lambda}{4} \phi \star \phi \star \phi \star \phi \right], \quad (3)$$

where the second term is the vulcanization term with $\tilde{x}^\mu \equiv 2(\theta^{-1})^{\mu\nu} x_\nu$, and the metric is Euclidean. Their conclusion was that one should change the free propagator to get a renormalizable NCQFT. The guideline (using Langmann-Szabo symmetry [5]) was to incorporate the mixing of ultraviolet physics with infrared physics in each order of the

*Electronic address: iycho@skku.edu

†Electronic address: youngone@daejin.ac.kr

perturbation. It was later proved in Ref. [6] that the value of the coupling constant Ω is not restricted. It simply needs to be any value which is nonzero positive.

If we require renormalizability as a guideline, additional terms in the noncommutative field theory action will be inevitable as we have seen in the vulcanization theory. In the classical limit ($\theta_{i=E,B} \rightarrow 0$), the action (3) takes the form,

$$S[\phi] = \int d^4x \sqrt{g} \left[\frac{1}{2} \partial_\mu \phi \partial^\mu \phi + \frac{\Omega^2}{2} \tilde{x}_\mu \tilde{x}^\mu \phi \phi + \frac{m^2}{2} \phi^2 + \frac{\lambda}{4} \phi^4 \right]. \quad (4)$$

The noncommutativity parameter θ_i is hidden in the vulcanization term,

$$\frac{\Omega^2}{2} \tilde{x}_\mu \tilde{x}^\mu \phi \phi = 2\Omega^2 \left[\frac{(x_E)^a (x_E)_a}{\theta_E^2} + \frac{(x_B)^a (x_B)_a}{\theta_B^2} \right] \phi \phi, \quad (5)$$

where $(x_i)^a$ is the coordinate corresponding to the electric/magnetic components in Eq. (2). When $\theta_i = 0$, the corresponding term in Eq. (5) is absent. The theory in the classical limit is now described by the parameter $\Omega_{\theta_i} = \Omega/\theta_i$, which is the ratio of the vulcanization and the noncommutativity parameters. Since Ω can be any positive value, we can always make Ω_{θ_i} be finite for any small θ_i . In this picture, the classical limit of the vulcanization theory is never the same with the ordinary classical action, so it is very interesting to study this limit. To understand this classical limit, it will be helpful to investigate classical objects in the presence of the vulcanization term.

Since the vulcanization term is coordinate-dependent, it is suggestive to consider an inhomogeneous field configuration resulting from the theory. Interesting candidates for such a configuration would be (non)topological solitons. In this article, we shall introduce a complex scalar field which is associated with global U(1) symmetry. The possible solitonic candidates are topological [7] or nontopological [8] vortices, and Q-ball type nontopological solitons [9, 10]. Topological solitons arise in the field theory of symmetry breaking. Their outer boundary takes the vacuum-expectation value in the broken-symmetry state. The vacuum is specified by a nontrivial homotopy group. This type of soliton is topologically stable since there is no continuous transformation that deforms them homotopically to a trivial solution. Nontopological solitons, on the other hand, can arise with the theory of unbroken symmetry. The outer boundary acquires the value of the vacuum which is not nontrivial homotopically. Their stability is provided by a conserved U(1) charge. They are usually the lowest-energy configuration of the theory.

We perform numerical calculations in order to see if there exist field configurations which satisfy boundary conditions for the various types of solutions above. In our model of the vulcanized theory, we find that there may exist nontopological vortices and Q-ball type solitons of which integrated energy is finite. However, the vortex solution which meets the topological boundary condition does not exist. In Sec. II, we present the setup of the vulcanization model with global U(1) symmetry. In Sec. III, we numerically search various (non)topological solutions for the field and analyze them. In Sec. IV, we conclude.

II. SETUP

In this section, we present a vortex model motivated by the vulcanized noncommutative theory. In order to consider a vortex configuration, we introduce a complex scalar field. Then the classical action (4) becomes

$$S[\phi] = \int d^4x \sqrt{-g} \left[-\frac{1}{2} \partial_\mu \bar{\phi} \partial^\mu \phi - \frac{\Omega^2}{2} \tilde{x}_\mu \tilde{x}^\mu \bar{\phi} \phi - \frac{m^2}{2} \bar{\phi} \phi - \frac{\lambda}{4} (\bar{\phi} \phi)^2 \right], \quad (6)$$

where the metric is now Lorentzian. We do not face any trouble which arises in the Wick rotation from Euclidean to Lorentzian since we shall consider only spatial noncommutativity in what follows. We keep the SO(2) structure only in the spatial part on the (x, y) -plane, i.e., $\theta_E = 0$ and $\theta_B = \theta$. Then there is a translational symmetry in the t - and z -directions, and a circular symmetry in the (x, y) -plane. This corresponds to the cylindrical symmetry in 3D space.

In the cylindrical coordinate system $\{t, z, \rho, \vartheta\}$, the field equation then becomes

$$\nabla_\mu \partial^\mu \phi = \left[-\frac{\partial^2}{\partial t^2} + \frac{1}{\rho} \frac{\partial}{\partial \rho} \left(\rho \frac{\partial}{\partial \rho} \right) + \frac{1}{\rho^2} \frac{\partial^2}{\partial \vartheta^2} + \frac{\partial^2}{\partial z^2} \right] \phi = \lambda \bar{\phi} \phi + m^2 \phi + 4\Omega_\theta^2 \rho^2 \phi, \quad (7)$$

where $\Omega_\theta = \Omega/\theta$.

For the vortex configuration, we shall consider both topological and nontopological solutions. The ansatz for such a field can be

$$\phi(t, \rho, \vartheta) = e^{i\omega t} e^{in\vartheta} f(\rho), \quad (8)$$

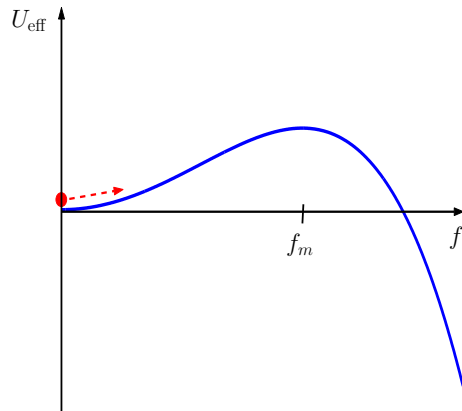


FIG. 1: Plot of the effective potential. The local maximum is at $f_m = \sqrt{(\omega^2 - m^2)/\lambda}$. For nontopological vortices, the field starting from zero with a finite velocity should come back to the original point with zero velocity and acceleration.

where $f(\rho)$ is the radial profile of the field, n is an integer representing vorticity, and ω is a number which is associated with the conserved U(1) charge. Since the model possesses global U(1) symmetry, there is a conserved Noether current $j^\mu = (i/2)[\bar{\phi}\partial^\mu\phi - (\partial^\mu\bar{\phi})\phi]$ whose charge is $Q = \int d^2x j^0 = \int d^2x \omega |\phi|^2$. While the stability of topological vortices is provided by the topological reason, i.e., nontrivial structure of the vacuum, that of the nontopological ones is provided by the conserved U(1) charge related with ω .

Plugging the ansatz (8) in the field Eq. (7), the field equation for the radial profile becomes

$$\left(\frac{d^2}{d\rho^2} + \frac{1}{\rho}\frac{d}{d\rho} - \frac{n^2}{\rho^2}\right)f = \lambda f^3 - (\omega^2 - m^2)f + 4\Omega_\theta^2\rho^2 f. \quad (9)$$

The vulcanization term is interpreted as a kind of source term, and the effective potential which constrains the field is given by

$$V_{\text{eff}} = V - \frac{\omega^2}{2}f^2, \quad \text{where } V = \frac{\lambda}{4}f^4 + \frac{m^2}{2}f^2 + V_0. \quad (10)$$

The constant V_0 is absent in the original action (6), but its introduction does not change the picture of the model. The value of V_0 simply shifts the magnitude of the vacuum energy which is indeed required to be zero for nontopological vortices.

III. SOLITON SOLUTIONS

In this section, we search soliton solutions of the field Eq. (9). In order to examine the existence of solutions for given boundary conditions, we treat the field equation as a dynamical one of which the solution is interpreted as the motion of the particle subject to the Newtonian equation. Then the field profile f means the position of the particle, and the radial coordinate ρ plays the role of time. The field Eq. (9) can be recast into the form

$$\frac{d^2 f}{d\rho^2} = -\frac{1}{\rho}\frac{df}{d\rho} + \frac{n^2}{\rho^2}f + \lambda f^3 - (\omega^2 - m^2)f + 4\Omega_\theta^2\rho^2 f, \quad (11)$$

where the left-hand side is acceleration and the terms on the right-hand side play a role of forces. The first term on the right-hand side is a friction proportional inversely to time, and the second term is a time-dependent repulsion which decays in time. The combination of the third and the fourth term is the conservative force subject to the effective potential $U_{\text{eff}} = -V_{\text{eff}}$. The last vulcanization term plays the same role with the second term (repulsive-force) but amplifies in time.

For right solutions, the motion subject to the effective potential U_{eff} shown in Fig. 1 (we need $\omega^2 > m^2$) and to the forces in Eq. (11), should meet the appropriate boundary conditions for soliton configurations. For soliton configurations, we consider topological vortices, nontopological vortices, and Q-ball type solitons which have different types of boundary conditions. We shall deal with them separately.

A. Topological vortex

The formation of topological vortices is associated with symmetry breaking. It is stable due to the topological reason and the frequency term is not required, $\omega = 0$. The corresponding potential is a Mexican-hat type given by the tachyonic mass, $m^2 < 0$. At the center of the vortex, the field stays at the symmetry state ($f = 0$), and approaches the broken-symmetry state ($f = |m|/\sqrt{\lambda}$) asymptotically.

For the topological vortex solutions with the boundary conditions above, the field starts from $f(\rho = 0) = 0$ with a finite velocity and should reach the top of the effective potential in Fig. 1, $f(\rho \rightarrow \infty) \rightarrow |m|/\sqrt{\lambda}$. At the top of U_{eff} , the acceleration and velocity should vanish. It is not difficult to see from Eq. (11) that this boundary condition cannot be met. With finite f and velocity $df/d\rho$, as ρ becomes large, the force terms approach zero except the vulcanization term which diverges. This makes the acceleration diverge, and the motion fails to meet the topological boundary condition.

More analytically, for vanishing acceleration ($d^2f/d\rho^2 = 0$) at the top of the potential ($\partial U_{\text{eff}}/\partial f = 0$), the field Eq. (11) and the solution to it become

$$-\frac{1}{\rho} \frac{df}{d\rho} + \frac{n^2}{\rho^2} f + 4\Omega_\theta^2 \rho^2 f = 0 \quad \Rightarrow \quad f = c_1 \rho^{n^2} \exp(\Omega_\theta^2 \rho^4). \quad (12)$$

It is easy to see that the solution is an increasing function of ρ and cannot reach a nonzero finite value asymptotically. Locally at a finite ρ one can have $f(\rho_*) = |m|/\sqrt{\lambda}$, but its velocity is nonzero there. As a result, the vulcanized noncommutative model does not admit a topological vortex solution.

B. Nontopological vortex

Nontopological solitons arise in the unbroken-symmetry theory [9, 10], and their stability is provided by the conserved U(1) Noether charge. The nontopological vortex, in particular, is an object produced in such a theory with vorticity [8]. For the nontopological vortex, therefore, both n and ω are turned on in the field ansatz (8), which indicates that there is a constant angular momentum. The boundary conditions for such a vortex are $f(\rho = 0) = 0$ and $f(\rho \rightarrow \infty) \rightarrow 0$; the field resides in the symmetry state in both boundaries. The shape of the field in the intermediate region between boundaries represents ringlike matter rotating about the center with an angular momentum.

Dynamically, the particle subject to the effective potential U_{eff} starts from $f(\rho = 0) = 0$ with some velocity and climbs up the hill. Then it has to turn back and to settle down at the original position $f = 0$ with zero acceleration and velocity at $\rho \rightarrow \infty$. From Eq. (11), as $\rho \rightarrow \infty$, the friction and the repulsion decay to zero. As $f \rightarrow 0$, the conservative force by U_{eff} becomes zero. The remaining vulcanization term $\propto \rho^2 f$ can also approach zero if f decays faster than $1/\rho^2$. The vulcanization term possibly provides the zero-acceleration boundary condition. However, the behavior of the velocity $df/d\rho$ remains undetermined. If we assume that f decays faster than $1/\rho^2$, the f^3 -term in Eq. (11) becomes most negligible. Then, there exists an approximate solution at large ρ ,

$$f(\rho) \approx \frac{c_1}{\rho} \text{WhittakerW} \left(\frac{\omega^2 - m^2}{8\Omega_\theta}, \frac{n}{2}, 2\Omega_\theta \rho^2 \right), \quad (13)$$

which decreases to zero rapidly as well as its velocity and acceleration. Therefore, it is very probable that there exists a vortex solution with nontopological boundary conditions. What is remaining is to check if this approximate large- ρ solution is obtained when the field equation is integrated from the core region with appropriate initial conditions. In order to see this, we need to perform numerical calculations.

For numerical calculations, we search the solution which approaches $f = 0$ asymptotically at large ρ with shooting at small ρ by tuning the velocity. In the vicinity of $\rho = 0$, the field can be expanded as

$$f(\rho) = f_1 \rho^n \left\{ 1 - \frac{\omega^2 - m^2}{4(n+1)} \rho^2 + \frac{1}{8(n+2)} \left[\frac{(\omega^2 - m^2)^2}{4(n+1)} + 4\Omega_\theta^2 + \lambda f_1^2 \delta_1^n \right] \rho^4 + \mathcal{O}(\rho^6) \right\}. \quad (14)$$

By varying f_1 we search the solution which satisfies the boundary conditions, $f \rightarrow 0$ and $df/d\rho \rightarrow 0$ at large ρ .

In order to satisfy the boundary conditions at both ends, the field f should increase first and then decrease. Before we perform numerical calculations, let us discuss necessary conditions for the turning of the field to have such a configuration. At the moment of turning, $\rho = \rho_t$, the velocity becomes zero, $(df/d\rho)(\rho_t) = 0$. The acceleration at this moment should be negative in order for the field to come back to the origin,

$$\left. \frac{d^2 f}{d\rho^2} \right|_{\rho=\rho_t} = \left[\frac{n^2}{\rho^2} f + \lambda f^3 - (\omega^2 - m^2) f + 4\Omega_\theta^2 \rho^2 f \right]_{\rho=\rho_t} < 0. \quad (15)$$

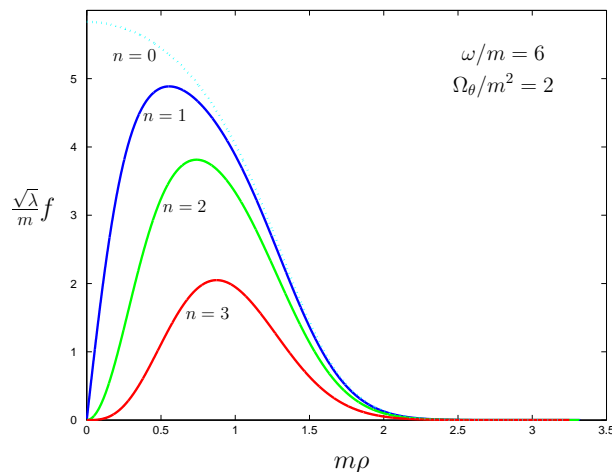


FIG. 2: Plot of the radial field profile of nontopological vortices for several winding numbers, and of Q-ball type solution ($n = 0$).

The solution to this inequality ranges as

$$0 < \sqrt{\lambda}f(\rho_t) < \sqrt{\omega^2 - m^2 - 4\Omega_\theta^2\rho_t^2 - \frac{n^2}{\rho_t^2}}. \quad (16)$$

First, note that the value of the field for the physical turning point is always smaller than the extremum value, $f(\rho_t) < f_m = \sqrt{(\omega^2 - m^2)/\lambda}$. The field which past the maximum of U_{eff} never returns. Second, in order to have a real solution for $f(\rho_t)$, the maximum value of the argument in the square-root in Eq. (16) should be positive. This gives a condition for the parameters,

$$\omega^2 - m^2 > 4n\Omega_\theta. \quad (17)$$

This is only a necessary condition for turning. With given initial conditions at $\rho = 0$, it is not analytically tractable to see whether or not the turning point $f(\rho_t)$ will be located in the range (16). We need to search numerically for the right solution which turns back and settles at the origin.

The numerical results for nontopological vortices are shown in Fig. 2 for $n = 1, 2, 3$. The field f increases initially with $f(\rho = 0) = 0$ and velocity determined by Eq. (14), and then turns to decrease. At large ρ , f approaches zero with decaying velocity to zero.¹ The decaying behavior is very close to the approximate solution given in Eq. (13).

In Fig. 3, we plotted several types of field configurations. Those configurations are obtained by varying the shooting parameter f_1 in Eq. (14).

- (i) When f_1 is very large [Case (b)], the field overcomes the maximum of U_{eff} and diverges to infinity.
- (ii) When f_1 is slightly larger than the nontopological one [Case (c)], the field turns back. However, the attractive force by ∂U_{eff} is soon overcome by the repulsive force. The field turns again and grows to infinity.²
- (iii) When f_1 is smaller than the nontopological one [Case (d)], the field returns to the origin, but with nonvanishing velocity. It passes the origin to the negative value, which becomes nonphysical.
- (iv) Between the configuration (c) and (d), we can always obtain the nontopological solution by finely tuning f_1 in principle.

The energy consideration helps one understand the dynamical description so far. We can define the total energy \mathcal{E} of the mechanical system as

$$\mathcal{E} = \frac{1}{2} \left(\frac{df}{d\rho} \right)^2 + U_{\text{eff}}. \quad (18)$$

¹ In order to obtain a long tail at large ρ for numerical solutions, a very fine-tuning for f_1 is required. It is mainly due to the vulcanization term which needs tail-down, but with an increasing coefficient $4\Omega_\theta^2\rho^2$ at large ρ .

² The solution cannot have more than two turning points. The proof is given in Appendix.

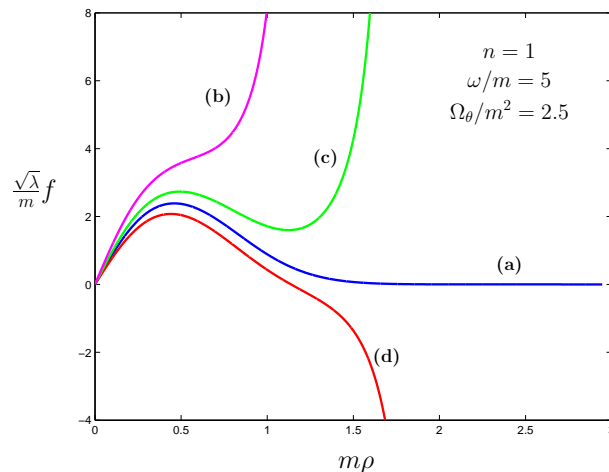


FIG. 3: Plot of numerical solutions for the radial profile with different shooting parameters (f_1). (a) Nontopological solution. (b) Solution for a much larger shooting parameter than the nontopological one. The solution monotonically increases without turning. (c) Solution for a slightly larger shooting parameter than the nontopological one. The solution returns before reaching the maximum of U_{eff} . However, the repulsive force mainly by the vulcanization term overcomes the attractive force, so the field starts to increase to infinity. (d) Solution for a smaller shooting parameter than the nontopological one. The field passes the origin with nonzero velocity.

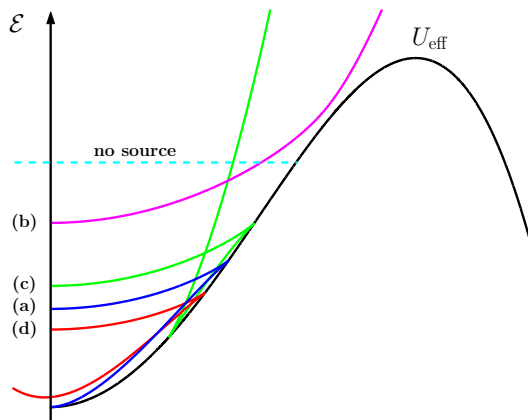


FIG. 4: Plot of \mathcal{E} vs f for the numerical solutions with the same parameters in Fig. 3. The solution (b) gains energy all the time and overcomes the potential barrier. The solution (c) exhibits two turning points ($\mathcal{E} = U_{\text{eff}}$) where the velocity becomes zero. The solution (d) passes the origin with nonvanishing kinetic energy. Between the solution (c) and (d), there exists a nontopological solution for which the latter $\mathcal{E} = U_{\text{eff}}$ occurs at $f = 0$.

This energy is not a conserved quantity and changes due to driving sources. With the aid of Eq. (11), the change-rate is given by

$$\frac{d\mathcal{E}}{d\rho} = -\frac{1}{\rho} \left(\frac{df}{d\rho} \right)^2 + \left(\frac{n^2}{\rho^2} + 4\Omega_\theta^2 \rho^2 \right) f \frac{df}{d\rho}. \quad (19)$$

The terms on the right-hand side are interpreted as sources. If there is no source at all, the energy is conserved and the system becomes an oscillator. (See Fig. 4.)

The first term in the right-hand side of Eq. (19) always extracts energy from the system. The second term adds energy to the system when f increases, and extracts energy when f decreases. Therefore, these two terms compete when f increase, and cooperate when f decreases. At the initial moment, the condition $f(\rho = 0) = 0$ implies that the potential energy is zero (by setting $V_0 = 0$ in Eq. (10)), and that the total energy \mathcal{E} is solely given by the initial

velocity.³ At small ρ , with f in Eq. (14), the change-rate can be expanded as

$$\frac{d\mathcal{E}}{d\rho} = f_1^2 n\rho^{2n-3} \left[n(n-1) - \frac{(n^2-2)(\omega^2-m^2)}{2(n+1)}\rho^2 + \mathcal{O}(\rho^4) \right], \quad (20)$$

which is positive for all n 's. Therefore, the total energy increases initially. Depending on the shooting parameter f_1 , the competition pattern between the two terms in Eq. (19) is different.

(i) When f_1 is large enough, the system always gains energy and the field f overcomes the maximum of U_{eff} at f_m owing to the acquired energy [Case (b)].

(ii) When f_1 is lowered, the energy gain is not very efficient, and the total energy \mathcal{E} becomes the same with U_{eff} before the field f reaches the maximum f_m [Case (c)]. The kinetic energy vanishes at that moment, and the velocity changes its sign afterwards. When f returns to the origin, the energy \mathcal{E} always decreases. If f_1 is not sufficiently low, \mathcal{E} hits U_{eff} again at $f > 0$, and f changes its direction. Finally, the field evolves similarly to that in (i).

(iii) When f_1 is considerably low, the system loses energy slowly during the returning of f , and the second turning point ($\mathcal{E} = U_{\text{eff}}$) does not arise in the region of $f \geq 0$ [Case (d)]. The field f passes the origin with nonzero negative velocity.

(iv) Tuning f_1 finely between those for (c) and (d), there exists a trajectory for which the $\mathcal{E} = U_{\text{eff}}$ point occurs at $f = 0$ [Case (a)]. The velocity vanishes there, $df/d\rho = 0$, and the acceleration becomes zero, $d^2f/d\rho^2 = 0$, as it was analyzed earlier. This will occur at $\rho \rightarrow \infty$ and one gets the nontopological vortex solution.

C. Q-ball type solution

The Q-ball is a nontopological soliton which was first investigated in [9, 10]. It possesses only the U(1) Noether charge, but no vorticity ($n = 0$). Here, we shall search a solution which satisfies the boundary conditions of the Q-ball type. Similarly to vortices, the radial profile of the field approaches asymptotically the symmetry state, $f(\rho \rightarrow \infty) \rightarrow 0$, but from a nonzero inner boundary value which is off the local extremum of U_{eff} , $f(\rho = 0) = f_m - \xi$. We try to search a numerical solution which satisfies these boundary conditions. For the inner boundary, we can perform a series expansion in the vicinity of $\rho = 0$,

$$f(\rho) = (f_m - \xi) - \frac{\lambda}{4}\xi(f_m - \xi)(2f_m - \xi)\rho^2 + \frac{\lambda}{64}(f_m - \xi) \left[-16\frac{\Omega_\theta^2}{\lambda} + 4(\omega^2 - m^2)f_m\xi - 14(\omega^2 - m^2)\xi^2 + 12\lambda f_m\xi^3 - 3\lambda\xi^4 \right] \rho^4 + \mathcal{O}(\rho^6). \quad (21)$$

Now, the shooting parameter is ξ . By varying ξ , we search a numerical solution which meets the outer boundary condition. Dynamical interpretation states that the field f starting from $f = f_m - \xi$ should settle down to the local minimum at $\rho \rightarrow \infty$. The numerical solution for $f(\rho)$ is plotted in Fig. 2, and the energy profile is plotted in Fig. 5. The asymptotic behavior of f approximates the analytic function (13) with setting $n = 0$. The existence of such a Q-ball type solution is very similar to that for the nontopological vortices explained based on Fig. 3. If ξ is a bit smaller than that for the Q-ball type solution, the field f , which decreases initially from $f_m - \xi$, turns and diverges to infinity. It is similar to Case (c) for vortices. If ξ is a bit larger, f decreases and passes $f = 0$ to negative similarly to Case (d) for vortices. Between them, there exists a Q-ball type solution.

For nontopological vortices and Q-ball type solitons, the integrated energy over the cross-sectional 2D space,

$$E = 2\pi \int_0^\infty d\rho \rho \mathcal{H}, \quad (22)$$

is finite, where the Hamiltonian density is given by

$$\mathcal{H} = \frac{1}{2}\nabla_i\bar{\phi}\nabla^i\phi + V + \frac{1}{2}\omega^2\bar{\phi}\phi + \frac{\Omega^2}{2}\tilde{x}_\mu\tilde{x}^\mu\bar{\phi}\phi = \frac{1}{2}\left(\frac{df}{d\rho}\right)^2 + \frac{n^2}{2}\frac{f^2}{\rho^2} + V + \frac{\omega^2}{2}f^2 + 2\Omega_\theta^2\rho^2f^2. \quad (23)$$

As it was mentioned earlier, in order to have zero acceleration at the outer boundary, f should decay faster than $1/\rho^2$. This guarantees that the integration of the above Hamiltonian density converges.

³ From the expression for f at small ρ given in Eq. (14), one can see that the initial velocity is nonzero only for $n = 1$ ($df/d\rho(0) = f_1$); the shooting parameter becomes the initial velocity for $n = 1$). Therefore, the initial energy is zero for $n \geq 2$.

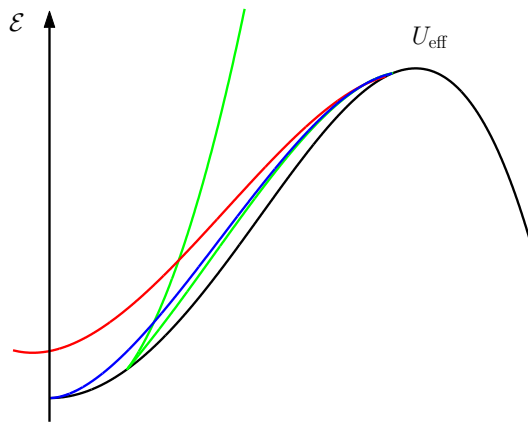


FIG. 5: Plot of \mathcal{E} vs f for Q-ball type solutions for $\omega/m = 5$ and $\Omega_\theta/m^2 = 2.5$. The blue line represents the solution which meets the boundary conditions of Q-ball type. If the shooting parameter ξ is a bit smaller (i.e., $f(0) = f_m - \xi > f_{\text{Q-ball}}(0)$), there exists a turning point and the field f diverges as in Case (c) for vortices. If the shooting parameter ξ is a bit larger, the field passes the origin as in Case (d) for vortices.

IV. CONCLUSIONS

In this article, we investigated solitonic configurations motivated by the vulcanized theory which was introduced to renormalize the ϕ_\star^4 noncommutative field theory. We studied the classical limit of the theory which is distinctly different from the ordinary one. The vulcanization term is always present in this limit, and is described by the parameter Ω_θ that is the ratio of the vulcanization parameter Ω and the noncommutative parameter θ . We set up a model of global U(1) symmetry described by a complex scalar field. Since the vulcanization term is x -dependent, we considered inhomogeneous field configurations such as vortices and Q-ball type solitons. We performed numerical calculations to find solutions to the field equation which satisfy boundary conditions for those configurations.

The result shows that there can form nontopological vortices and Q-ball type solitons, but no topological vortices. Because of the vulcanization term, the radial profile of the scalar field cannot approach a nonzero constant value asymptotically, so it cannot acquire the nonzero vacuum-expectation value at the boundary. However, the field can approach the nontopological boundary value which represents the unbroken-symmetry state. This was possible with the aid of the vulcanization term with ϕ^4 -potential in the absence of the ϕ^6 term which plays the major role in the usual nontopological solitons. The $n = 0$ solution corresponds to the Q-ball type solution. The $n \neq 0$ solutions correspond to the nontopological vortex which has a constant angular momentum.

The integrated energy of nontopological vulcanized solitons is finite. Since physics of the vulcanized field theory has not been completely studied yet, identification of the objects that resulted from the theory with the physical objects (e.g., meson) is incomplete. Therefore, whether or not the nontopological vulcanized solitons are the lowest-energy objects in the theory is not yet manifest. It is too early to discuss their stability or decay, and needs further investigation.

The nontopological solitonic objects that we obtained here are realized as stationary stringlike objects in 3D space in the Universe. Our results can be applied to the stage in the early universe where the renormalizable noncommutativity still works and its classical limit is also viable. We expect that the cosmological implications of our solutions would not be much different from those in the usual commutative theory [11].

Acknowledgments

The authors are grateful to Yoonbai Kim and Hiroaki Nakajima for useful discussions. Y.L. was supported by the Korea Research Foundation Grant (KRF-2008-314-C00063) funded by the Korean Government (MOEHRD).

APPENDIX: PROOF OF NO MULTI-HUMP SOLUTION FOR f

Here we prove that there is no solution to (11) which has more than two local maxima in $f(\rho)$.

Proof) Let $f(\rho)$ be a solution that has two local maxima at $f_1 = f(\rho_1)$ and $f_3 = f(\rho_3)$, and one local minimum at

$f_2 = f(\rho_2)$ ($\rho_1 < \rho_2 < \rho_3$), i.e., $f_2 = \min(f_1, f_2, f_3)$. From Eq. (15), the local maximum/minimum condition can be written as

$$\lambda f_1^2 < R(\rho_1), \quad \lambda f_3^2 < R(\rho_3), \quad \text{and} \quad \lambda f_2^2 > R(\rho_2), \quad (\text{A.1})$$

where $R(\rho) \equiv \omega^2 - m^2 - 4\Omega_\theta^2 \rho^2 - n^2/\rho^2$, and we consider only $f(\rho) > 0$. Since $R(\rho)$ is convex in ρ , $R(\rho_2)$ is always larger than at least one of the others, $R(\rho_2) > R(\rho_1)$ or/and $R(\rho_3)$. Therefore, from (A.1))

$$\lambda f_2^2 > R(\rho_2) > R(\rho_1) \text{ or/and } R(\rho_3) > \lambda f_1^2 \text{ or } \lambda f_3^2. \quad (\text{A.2})$$

However, this inequality is against the initial assumption $f_2 = \min(f_1, f_2, f_3)$ which tells that f_2 is the local minimum.

- [1] S. Doplicher, K. Fredenhagen and J. E. Roberts, *Commun. Math. Phys.* **172**, 187 (1995) [arXiv:hep-th/0303037].
- [2] J. Lukierski, H. Ruegg, A. Nowicki and V. N. Tolstoy, *Phys. Lett. B* **264**, 331 (1991); J. Lukierski and H. Ruegg, *Phys. Lett. B* **329**, 189 (1994) [arXiv:hep-th/9310117]; S. Majid and H. Ruegg, *Phys. Lett. B* **334**, 348 (1994) [arXiv:hep-th/9405107].
- [3] S. Minwalla, M. Van Raamsdonk and N. Seiberg, *JHEP* **0002**, 020 (2000) [arXiv:hep-th/9912072].
- [4] H. Grosse and R. Wulkenhaar, *Commun. Math. Phys.* **256**, 305 (2005) [arXiv:hep-th/0401128].
- [5] E. Langmann and R. J. Szabo, *Phys. Lett. B* **533**, 168 (2002) [arXiv:hep-th/0202039].
- [6] R. Gurau, J. Magnen, V. Rivasseau and F. Vignes-Tourneret, *Commun. Math. Phys.* **267**, 515 (2006) [arXiv:hep-th/0512271].
- [7] For a review, see, for example, A. Vilenkin and E. P. S. Shellard, *Cosmic strings and other topological defects*, (Cambridge University Press, 1984); N. Manton and P. Sutcliffe, *Topological solitons*, (Cambridge University Press, 2004).
- [8] C. j. Kim, S. Kim and Y. b. Kim, *Phys. Rev. D* **47**, 5434 (1993).
- [9] R. Friedberg, T. D. Lee and A. Sirlin, *Phys. Rev. D* **13**, 2739 (1976); S. R. Coleman, *Nucl. Phys. B* **262**, 263 (1985); *B* **269**, 744(E) (1986).
- [10] For a review see, for example, T. D. Lee, *Particle Physics and Introduction to Field Theory*, (Harwood Academic, Beijing, 1981).
- [11] T. D. Lee, *Phys. Rev. D* **35**, 3637 (1987); R. Friedberg, T. D. Lee and Y. Pang, *ibid.* **35**, 3640 (1987); J. A. Frieman, G. B. Gelmini, M. Gleiser and E. W. Kolb, *Phys. Rev. Lett.* **60**, 2101 (1988); B. A. Gradwohl, *Phys. Rev. D* **44**, 1685 (1991).